Fire behaviour of composite materials using kerosene burner tests at small-scales

Eliot Schuhler, Avinash Chaudhary, Benoît Vieille, Alexis Coppalle

Fire behaviour of composite materials using kerosene burner tests at small-scales

E. Schuhler[a], A. Chaudhary[a,c], B. Vieille[b], A. Coppalle[a]

a Normandie Univ, UNIROUEN, INSA Rouen, CNRS, CORIA, 76000 Rouen, France
b Normandie Univ, UNIROUEN, INSA Rouen, CNRS, Groupe de Physique des Matériaux, 76000 Rouen, France
c School of Mechanical Engineering, KIIT University, Bhubaneswar, India

Nomenclature

h	Convective heat transfer coefficient of the flame	$W/m/K$
h_{cv}	Convective heat transfer coefficient with ambient air	$W/m/K$
T	Temperature	K
$L_{T,\lambda}$	Black body spectral luminance	$W/sr/m^2/\mu m$
ε	Emissivity	-
λ	Wavelength	μm
Φ_r	Radiative heat flux	W/m^2
Φ_0	Total heat flux	W/m^2
σ	Stephan-Boltzmann constant	$W/m^2/K^4$

Abstract

In order to study fire behavior of composites used in the aeronautic field, a kerosene-flame burner has been designed and built allowing to thermally stress one side of small samples with a flame, reproducing the scenario of an engine fire. The burner has been optimized to obtain the same conditions as in standard tests, flame temperature of 1100°C and heat flux of 116 kW/m^2. During the tests, the temperature of the rear face is measured with an infrared camera, and the mass loss with a weighting cell. An original method has been developed in order to determine the convective coefficient of the flame on the composite samples as well as the contribution of the radiative part of the total heat flux. It uses the thermal balance of a thin steel plate heated by the flame. The bench test was used to analyze the fire behavior of two carbon fiber reinforced polymer composites, a first one with thermosetting matrix (epoxy 8552) and a second with a thermoplastic matrix (polyphenylene sulfide). The results are shown and analyzed. The comparison will highlight the main differences observed in terms of fire resistance.

https://doi.org/10.1016/j.firesaf.2021.103290

1. Introduction

Composite materials are now widely used in transportation systems. In particular in aeronautic, as a malfunction of the engines or after a crash, they may be exposed to a kerosene flame. Then the composite is decomposed, it loses its mechanical performances or under certain circumstances fuselage burn-through may occur with high risk for passengers. The behaviour of composites in fire has been the subject of much work. Many publications dealing with this topic are available, as for example the state of art given by Mouritz and Gibson [1].

In order to test the fire resistance of the materials, several standard tests specific to aeronautical applications are commonly used [1]. In particular, two different types of burner are described in the international standards for civil aircraft fire resistance [2], [3], one type of burner using propane as fuel and the other type using kerosene. The standard tests are mandatory for material qualification and a few research programs are carried on these standard burners. In particular, Le Neve [4] points out differences on the qualification results depending on the burner type used to perform the test. More recently, Hörold et al. [5] have shown that they can also be used to perform mechanical tests under thermal decomposition. However, the standard burners are not intended to provide results allowing to analyze and understand the processes of thermal decomposition. Moreover, the realization of full-scale tests is costly, time consuming and requires heavy equipment. For research and development of optimized composite materials, it is interesting to perform tests at smaller scale, typically with sample size of a dozen of centimeters. More refined experimental setup can be installed and analyses can be done on a large number of samples, for comparing the fire resistance of the different materials. The observations and the obtained experimental data are also required to validate modeling tools, useful for designing new materials [6].

Even though flame exposure presents multiple advantages, so far, most of the laboratory scale studies are performed with a cone calorimeter to apply a radiative heat flux on the sample [7], [8]. However, a direct flame impact is a more realistic thermal stress and heat flux greater than 100 kW/m^2 can be easily reached for a lot of fire scenarios. Since the 2010's, a large number of research programs are carried out on in-house developed propane burner [9]–[12]. Aims of the present study are multiple. The first goal is to show the feasibility of developing a small kerosene burner for laboratory tests. The second is to present a simple method to measure the radiative contribution in the wall heat flux, which is different in the propane and kerosene burners. It has been observed that differences appear when comparing propane and kerosene certification burner [4]. This simple method has been applied to the kerosene burner. The last goal is to provide an example and to highlight the usefulness of this bench test to analyse fire behaviour, results obtained for both a thermoplastic and a thermoset composite are presented.

For the results presented here, the kerosene and air flow rates have been optimized in order to obtain similar flame conditions as in the standards [2], [3]. At the sample location, flame temperature is 1100 °C and the heat flux 116 kW/m^2. The temperature on the back face has been measured with an infrared camera, and the mass loss of the sample has been monitored during tests.

First, the burner design and the flame characteristics are presented. Details are given on the sample holders and measurement systems. Then, results for a special test on a thin steel plate will be shown and analyzed. It has been made in order to determine the convective coefficient of the flame on the composite samples as well as the radiative part of the heat flux. Finally, the results for two carbon fiber reinforced polymer composites, a thermosetting based (epoxy 8552) and a thermoplastic based (polyphenylene sulfide), will be shown and analyzed. The comparison will highlight the main differences observed in term of fire resistance.

2. Materials and experimental set-up

2.1 Materials and specimens

The composite materials studied in this work are carbon/epoxy and carbon/polyphenylene sulfide **(**PPS) woven-plies laminates. The samples are 70x70 mm^2, they are cut from prepreg laminate plates.
The thermoplastic-based laminates (C/PPS) are seven plies carbon-fiber reinforced PPS prepreg laminate. The PPS resin and the carbon fibers (T300 3K 5HS) are respectively supplied by Hexcel and Toray [13]. The mass fraction of carbon fiber is 58 %. The glass transition temperature of the material is T_g=98 °C and its melting temperature T_m=280 °C, as measured by DSC [14]. The crystallinity of PPS matrix is close to 30 %. The laminates thickness is 2.2 mm and the onset of thermal degradation is about 493 °C. The thermosetting-based laminates (C/epoxy) are referred to as AcF2 [15]. The glass transition temperature is about 190 °C and the peak of thermal degradation is about 390 °C as shown in Fig. 1.

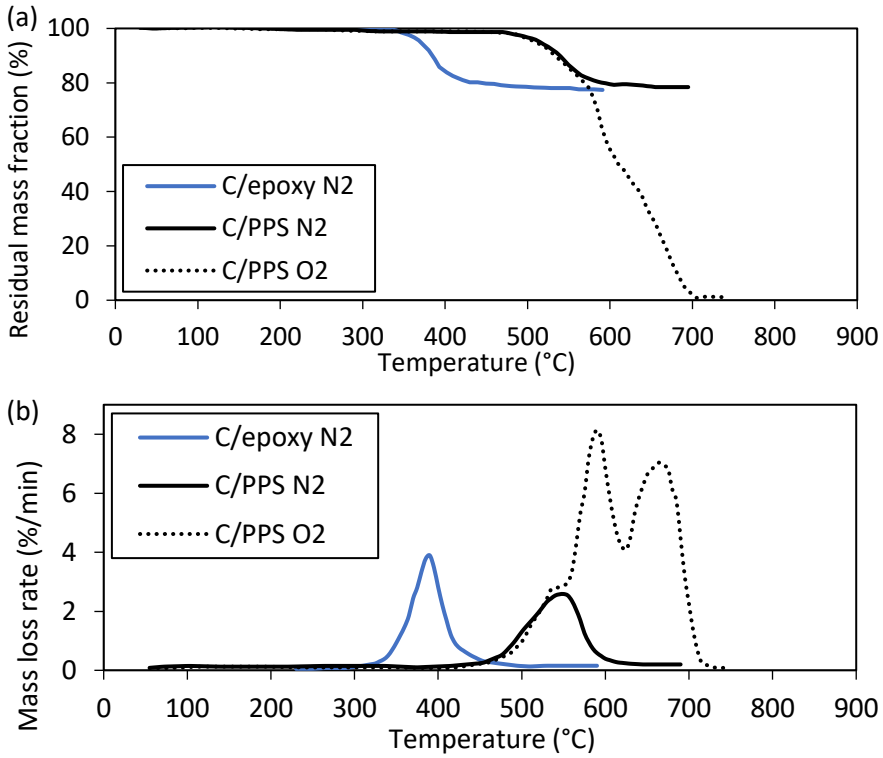

Fig. 1. (a) Residual mass and (b) mass loss rate for TGA at 10K/min for C/PPS [13] and C/epoxy [15].

2.2 Experimental set-up

2.2.1 Kerosene burner bench

The burner shown in Fig. 2 is made with a domestic device (Cuenod manufacturer). The kerosene is injected in a nozzle generating a hollow cone spray with an angle equal to 80° and a maximum flow rate of 0,3 g/s. This flow rate is controlled with a mass flow meter (MINI CORI-FLOW™, Bronkhorst), and it can be adjusted. Airflow is also controlled with a mass flow meter (EL-FLOW® Prestige, Bronkhorst).
The air to fuel ratio has been selected at 0.85 of the stoichiometric value, in order to obtain heat flux and temperatures values close to the standard values (116 kW/m^2 and 1100°C) at the sample location. The flame at the exit of the turbulator is a wide and turbulent jet. Therefore, a 50 mm diameter steel tube is installed after the turbulator to channel the hot combustion gases on the exposed area of the sample. Detail of the setting is presented Fig. 2. With this design, an efficient mixing occurs inside the first part of

the flame tube, and in its remaining part, the flow turbulence is strongly damped. At the flame tube exit, no kerosene droplets are observed and the combustion is completed. Thus, the thermal stress on the sample is due to the hot gas mixture of the combustion products [13]. The flame tube diameter is chosen equal to the diameter of the sample exposed surface. Thus, the hot gas stream close the sample wall corresponds to the stagnation zone of an impinging jet and the wall heat flux is nearly constant, as shown in a previous work on propane burner [16].

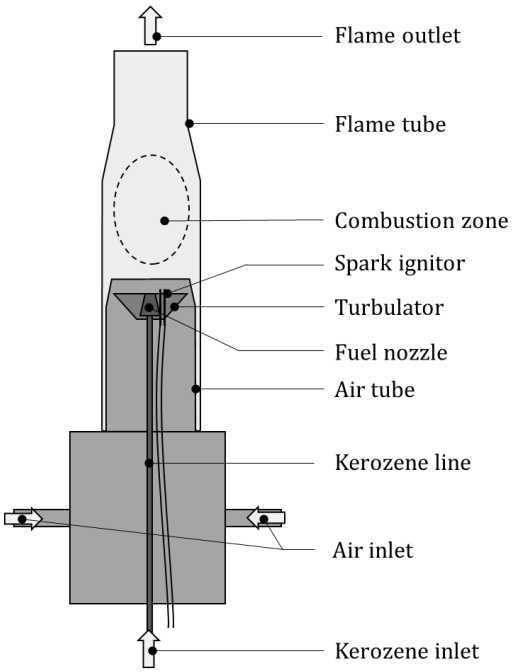

Fig. 2. Scheme of the laboratory scale kerozene burner.

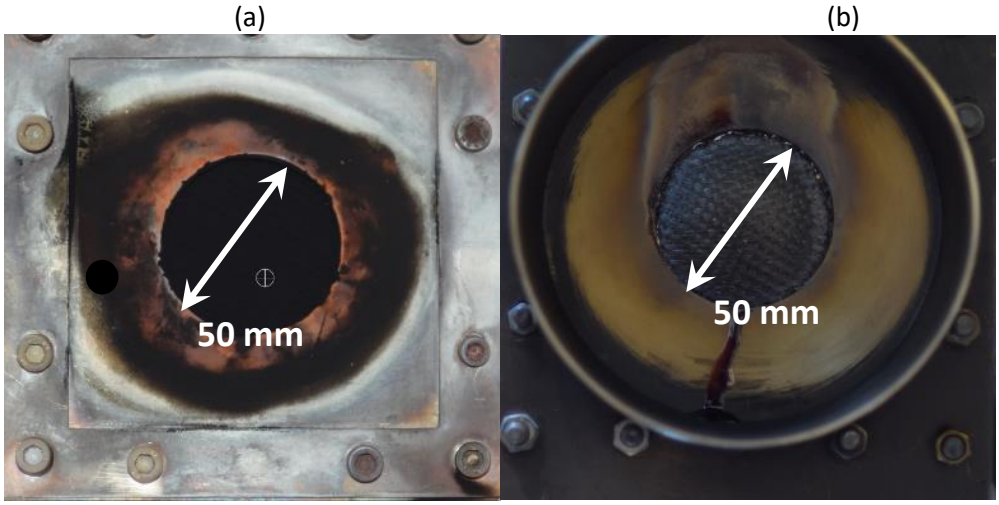

Fig. 3. Observations of the sample holder: (a) exposed face – (b) back face.

The composite samples described in section 2.1 are placed in a dedicated sample holder for the test. The sample holder is presented in Fig. 3. The composite sample is placed between two insulation layers and the assembly is clamped by two steel plates. In both side of the sample holder a round window of 50 mm diameter is made. On the front side, the sample is facing the burner output, on the back side, the temperature measurement is performed. This sample holder with an insulation have two major aims. The

first one is to prevent the surrounding of the sample by the flame. The second one is to maintain the integrity of the sample border. Maintaining the integrity of the sample border may be of great interest to perform further investigation combining the kerosene burner and a mechanical load. The 50 mm diameter is chosen in order to maintain a uniform heat flux on the exposed sample surface while maintaining at least 10 mm on the sample border.

2.2.2 Temperatures measurement

The temperature of the rear face of the samples has been measured using an IR camera (ThermaCam PM595). The camera works on the wavelength range 7.5-13 µm, it is equipped with a filter allowing temperature measurement between 80 and 500 °C. The IR camera is placed at 800 mm from the sample holder to avoid the hot gas flow. The IR camera allows a temperature measurement on the whole sample surface to analyze the homogeneity on the rear surface with an accuracy of ± 2°C. However, this method presents a major drawback as it is extremely difficult, during tests, to know the surface emissivity. In the present work, the emissivity is assumed to be constant and equal to 0.9. This corresponds to a common value used in the literature for this type of work [17], [18]. The chosen value corresponds to the carbon fiber emissivity measured by Balat-Pichelin et al. [19] it is also close to the value measured on virgin and degraded carbon epoxy laminate up to a temperature of 400°C [20], [21].
The sample holder is vertical and fixed to an insulating plate, and the assembly rests on a weighting cell (Mettler Toledo). With this layout, the effect of the hot impinging jet on the mass loss measurement is negligible since it acts as a force perpendicular to the sample holder weight. The weighting cell is protected by an insulation fiberboard, and its readability is 0.01 g.

3. Results and discussion

3.1 Control of the thermal stress applied to the samples

Before each test, the temperature and heat flux measurements are carried out in the hot gas jet, at the same distance from the exit of the flame tube as the sample holder. The temperature is measured using a mobile comb of 6 K type thermocouples, the spacing between each thermocouple being 8 mm, as shown in Fig. 4. After the burner ignition, a period of fifteen minutes is necessary in order to reach steady conditions in temperature, as shown in Fig. 5.

Fig. 4. (a) Observation of the free kerosene jet flame exiting the flame-tube, the flux meter inserted into a steel plate. (b) Observation of the movable rows of 6 type K thermocouples.

There is no major difference between the four thermocouples in the center of the jet, however one can see 200 °C difference with the two thermocouples located at the edge. This temperature difference is greatly reduced when the measurement is made just below the sample as shown in a previous work [9]. After the thermocouple comb is removed, the heat flux is measured using a water-cooled heat flux sensor

[22], [23] (Captec manufacturer) inserted into a movable steel plate, as shown in Fig. 4. The value is monitored during a few minutes, and it is well stable as shown in Fig. 5. Finally, the heat flux sensor is removed and the sample holder is translated in front of the flame.
For all the tests presented here, the mean value of the temperature at the center of the hot jet is 1080 ±30 °C. For the heat flux, the mean value is 120 ± 5 kW/m^2. After the measurement of the flame conditions the sample is exposed to the flame for 900 s.

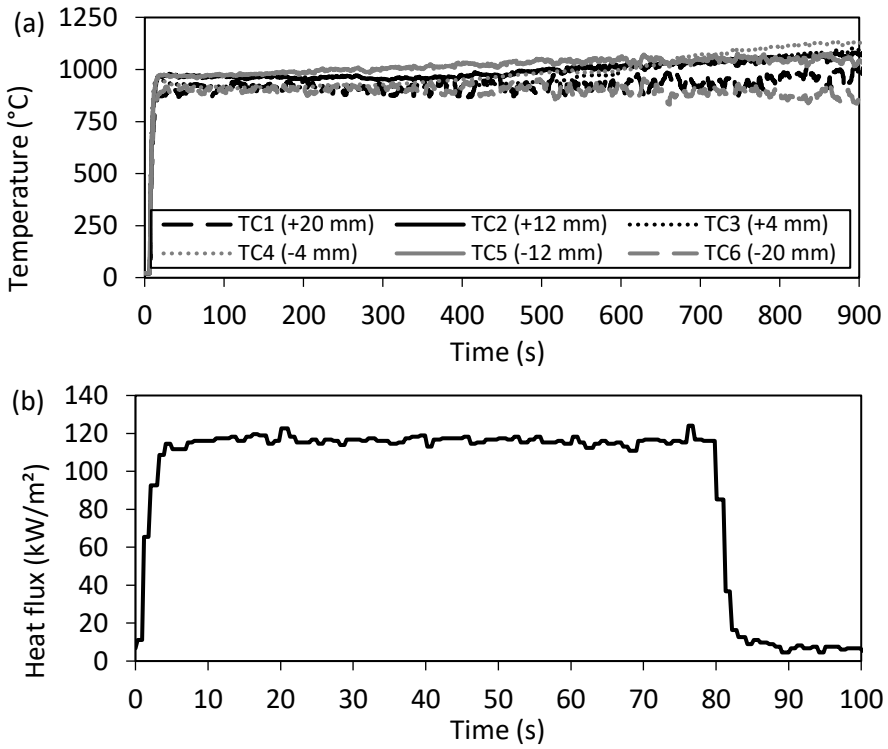

Fig. 5. (a) Temperature and (b) heat flux measurements before C/PPS test (PPS-III).

3.2 Heat transfer between the flame and the samples

The net heat flux on the surface facing the flame is the sum of the convective part h (T_f -T_s) and the radiative part ε Φr – ε σ T_s^4, with Φr the radiative flux incoming from the flame. During the exposure to the flame, the net heat flux decreases due to the increase of the surface temperature Ts. For a given Ts value, the higher the incoming radiative flux Φr, the higher will be the net heat flux, increasing the damage inside the material. Therefore, a good knowledge of the heating condition is necessary.
The flame produces a wall heat flux with a different radiative flux Φr depending on the nature of the fuel. In the case of a non-sooting flames, like the one produced by a gas burner supplied in stoichiometric conditions, the convective flux is important. With a kerosene flame, the soot production is higher, which increases the contribution of the radiative flux. Thus, it is interesting to consider the contribution of the radiative flux to the total flux on this specific test bench.
There have been many works dealing with the heat flux measurements on a wall. In the case of a high-temperature source like flames, the most popular are: the direct measurement using a heat flux sensor as Gardon gauge [16], [22], [23], or the temperature measurements of a heated plate. Various methods using a heated plate can be encountered, methods referred as plate thermometer [24], [25] or slug calorimeter [12] are using 1D thermal analysis. Other inverse methods are using 2D thermal analysis [26].
In the present study, a thermally thin steel plate (0.9 mm thickness) is used with one side exposed to the flame jet, and with a K-type thermocouple welded on the rear face as shown in Fig. 6. It is assumed that the heat transfer inside the thin plate is one dimensional through the thickness. With the IR camera, it has

been observed in the plate center that the radial temperature gradient is never greater than about 50 °C/cm. A simple energy balance in the radial and transverse directions shows that the thermal conduction heat flux in the radial direction is negligible compared to the heat flux provided by the flame. So, the steel plate energy balance, when reaching the thermal steady state, is given by the equation (1):

$$h\,(T_f - Tsp) + \varepsilon\,\Phi r = 2\varepsilon\,\sigma Tsp^4 + h_{cv}\,(Tsp - T_{amb}) \quad (1)$$

On the left side of the equation, h represents the convection coefficient of the impinging hot jet, Φr the radiative flux at the wall plate and ε the steel emissivity. On the left side, h_{cv} is the natural convection coefficient with the ambient air. T_f, Tsp and T_{amb} are respectively the temperatures of the flame, steel plate and ambient.
With the water-cooled heat flux sensor, the equation (2) is obtained:

$$\Phi_0 = h\,(T_f - T_{amb}) + \varepsilon_{FM}\,\Phi r \quad (2)$$

Where Φ_0 is the measured heat flux value, and ε_{FM} the emissivity of the sensor surface (manufacturer value is 0.94). The two main parameters that characterize the wall heat flux on the flame side are the convective coefficient h and Φr the radiative heat flux. They are unknown and the resolution of eqs. 1-2 provides the values, using the temperature measurements, T_f, T_{sp} and T_{amb}, T_{ps} being given by the welded thermocouple on the rear face.
However one has to know also the steel emissivity ε, which is a function of the wavelength, temperature and oxidation state [27]. It is estimated from a temperature measurement obtained with the IR camera, focused at the zone on the steel plate on which the thermocouple is welded. Assuming a guess value of the emissivity ε*, the IR camera provides the temperature T*. Thus, the true emissivity ε must satisfy equation (3).

$$\varepsilon \int_{\Delta\lambda} L^0_{T_{sp},\lambda}\,d\lambda = \varepsilon^* \int_{\Delta\lambda} L^0_{T^*,\lambda}\,d\lambda \quad (3)$$

with Δλ the spectral band width of the IR camera (7.5-13 μm).
The parameters h and Φr have been determined from three different tests. For the steel plate, the average value of the emissivity and the temperature are 0.22 and 991 K respectively, and the average flame conditions are T_f =1338 K and Φ_0 =117 kW/m². In order to calculate the natural convection coefficient h_{cv} on the rear face, the Churchill's law has been used [28]. With properties of ambient air, the Nusselt value is 48,3 giving h_{cv} equal to 12,55 W/m/K. Values of h and Φr have not been determined by averaging the solutions of the eqs 1-2 provided by each test, indeed they are given by the optimum values minimizing the total error on the three tests when resolving eq. 1 and 2. With this procedure, the value of h is found to be 52.5 W/m/K, which is corresponding to a local maximum at the stagnation point of the impinging flame jet [14]. The radiative heat flux Φr is found to be 66 kW/m². This last value means that the radiative flux is equal to 56 % of the total heat flux when the thermal steady state is reached. Thus, the radiative and convective fluxes have about the same contribution with this kerosene-flame test bench. As a comparison, previous measurements made on a propane burner working in similar conditions show a radiative heat flux Φr = 23.5 kW/m² [16] representing 22 % of the total flame heat flux.

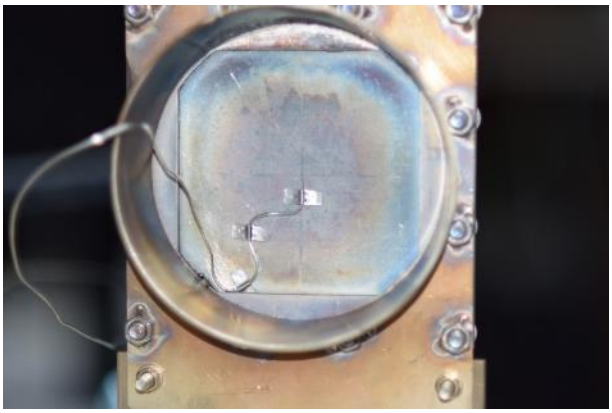

Fig. 6. Rear face of the steel plate with the welded thermocouple at the center.

3.3 Observation and analysis of the thermal decomposition of composite samples

Fig. 7 shows the faces of the samples before and after 900 s exposure to the kerosene burner. For both composites, the fibers at the front face are dry, and the polymer matrix is severely degraded on the back face. In C/PPS composites, some traces of degraded resin (char) are still visible. Swelling at the back faces is observable, more important in the case of thermoplastic-based composites. The geometry of the sample holder prevents the complete delamination of the sample.

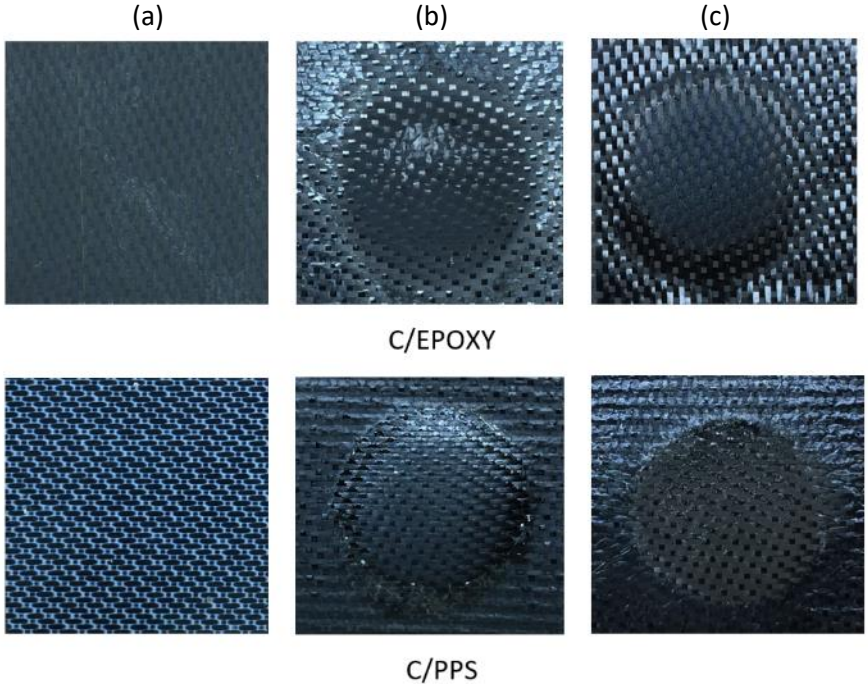

Fig. 7. Macroscopic observations of the C/epoxy and C/PPS samples, before and after 900 s exposure to the kerosene burner: (a) before test - (b) front face after test - (c) back face after test.

Mass losses are given in Fig. 8, the results are presented in percentage of the initial mass, i.e. the ratio of the mass at time t to the initial mass. The three tests carried out with the same composite (C/PPS or C/epoxy) allows to assure that the tests performed on this set up are repeatable. The greater differences

are found after 100 s for the thermosetting-based composite and after 600 s for the thermoplastic-based composite. The differences can be explained by internal damage mechanisms such as the building of cracks, delamination and major pores, that may be different from one test to another even with similar thermal stress. In other laboratory-scale studies using cone calorimeter [7] or a propane burner [9] mass loss has been measured and such variations between tests have also been found. However previous studies performed at large scale with a kerosene burner do not present mass loss results.
For the C/epoxy laminate, two different stages can be observed. First, there is substantial and rapid mass loss until 150 s followed by a slower decrease. In comparison, on the C/PPS laminate, the two stages are less pronounced and the mass is gradually decreasing with a slight change after 550s. The final mass loss is also different, respectively 68 % and 80% for the C/epoxy and C/PPS. These different behaviors between C/epoxy and C/PPS composites have been already investigated in previous work [9], using a propane burner. Zhang et al. have studied the thermal degradation of the /PPS composite (AcF2) using a cone calorimeter, they also found a faster mass loss and a greater final value compared to a PEEK thermoplastic-based composite [15]. The values of the onset temperature of degradation Td may explain the difference observed in Fig. 8, Td = 390 °C and 493 °C for the epoxy and PPS based composites respectively.

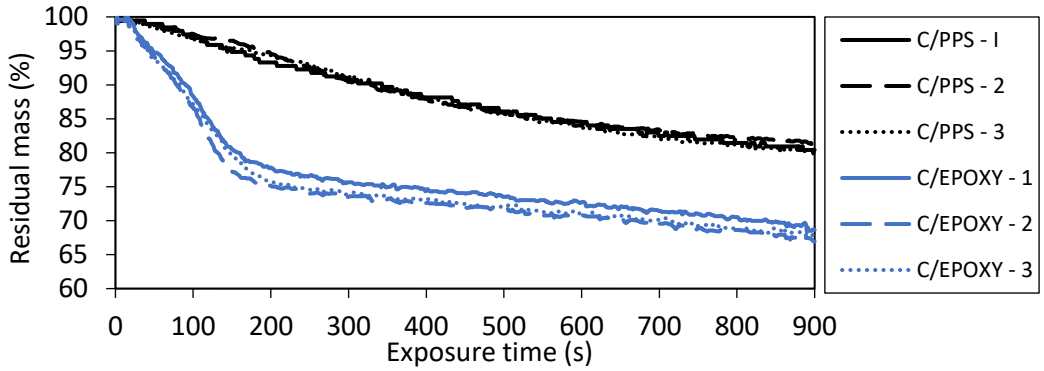

Fig. 8. Mass loss (in % of the initial mass) during thermal decomposition of C/PPS and C/epoxy samples, the thermal stress conditions are the same, 1089 °C and 120 kW/m2.

In *Fig. 9*, the temperature measured on the rear face with the IR camera are given for one C/PPS sample (C/PPS-3). At the beginning of the test, for time less than 200 s, there is no strong variation over the entire surface of the sample. This temperature homogeneity indicates that the heat flux on the exposed surface is rather constant, as shown in the ref [16] and that the heat transfer occurs mostly through the thickness. At the end of the test, temperature gradients can be observed on the surface. After 200s, the temperatures are greater than Td, the onset of thermal decomposition, cracks and delamination occur inside the material, changing the heat transfer through the sample. This is confirmed by the swelling observed on the rear face at the end of the test.

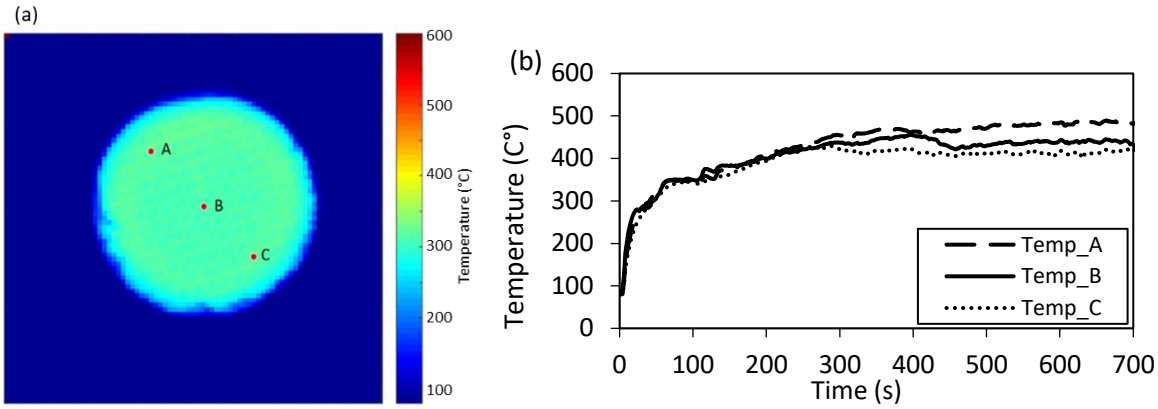

Fig. 9. Temperatures measured with the IR camera on the rear face of one C/PPS sample (PPS III): (a) snapshot of temperature distribution after 52 s, (b) temperature as a function of time for the three points A-B-C.

On Fig. 10, temperature variations averaged over a circle of diameter 6 mm on the center or the rear face are shown as a function of time, for C/PPS and C/epoxy samples. Up to about 10 s, there is a fast temperature increase with the same rate for both materials, about 750 K/minute. This suggests the existence of a strong thermal flux by conduction through the thickness and high temperature gradients, leading to high thermally-induced mechanical strains and resulting in micro-cracks formation and debonding between plies. After 10 s and for the thermoset, the temperature values drop significantly, which is due to occurrence of large cracks inside the sample acting as a thermal barrier. This phenomenon does not occur with the same intensity for C/PPS, for which one observes a rather slight variation in the growth of the temperatures.

At the end of the tests, a stationary thermal state is reached. Two processes compete at the exposed face of the samples. Due to the increase of the wall temperature, the flame convective flux is decreasing and the radiative heat loss is increasing. At the end of the test, an equilibrium between the two processes on the exposed face is reached. The temperature in C/PPS composites is lower than the one measured in C/epoxy composites. This suggests that, for this last material, the degradation is stronger and more complete due to its lower onset temperature of thermal decomposition (390°C for epoxy and 480°C for PPS). This is confirmed by looking at the rear face of the C/PPS composite (Fig. 7) showing that there is some degraded resin (or char) left at the end of the test. Likewise, a swelling is observed on the rear face of the C/PPS composites, much more compared to the thermosetting-based material, indicating that the delamination and the debonding of the plies are much more important, inducing a stronger thermal barrier effect as already shown in a previous work [9].

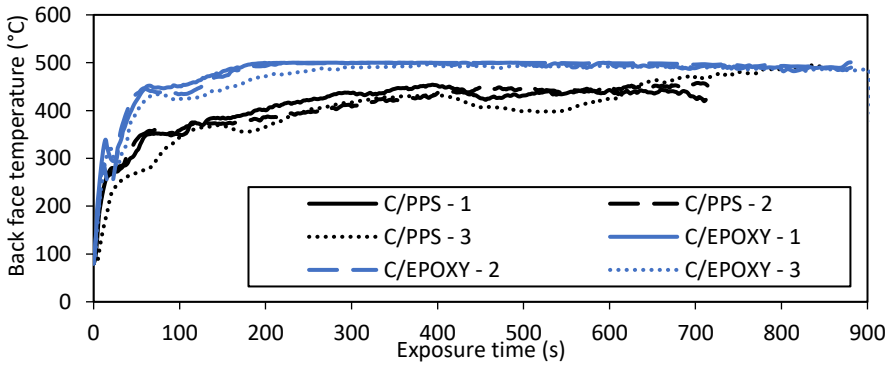

Fig. 10. Center-temperature variations on the rear face as a function of time, for the thermoplastic- and thermosetting-based samples.

4 Conclusion

A kerosene-flame test bench has been developed at laboratory scale in order to analyze and compare the fire behavior of composites, mainly for aeronautic applications. The kerosene and air flow rates have been chosen in order to produce similar thermal-stress conditions as in the standards [2], [3], a flame temperature equals to 1100°C and heat flux of 120 kW/m^2. During the test duration (15 min), the mass loss of the sample and the temperature on the back face are measured. Using a simple and original method, the radiation contribution to the total heat flux has been determined and is found equal to 56 %. Thus, the radiative and convective fluxes have about the same contribution with this kerosene-flame test bench. As a comparison, previous measurements made on a propane burner working in similar conditions show a radiative heat flux Φr = 23.5 kW/m^2 [16] representing 22 % of the total flame heat flux. This difference may have as consequence a more severe net heat flux on the exposed surface in the case of the kerosene flame.
With this device, it has been possible to analyze and compare the fire behavior of two carbon fiber reinforced polymers, a thermosetting-based one (C/epoxy) and a thermoplastic-based one (C/PPS), with the same thickness and the same stacking sequence.
Three tests have been carried out for each material, and a good repeatability has been found. Both the thermal decomposition and the mass loss show different as a function of time. The thermosetting-based laminate is decomposed very fast and reach higher final temperature at the back face. After 15 minutes, the thermoplastic-based composite is not fully decomposed and a significant swelling is observed, which seems to induce an important thermal protection effect.

Due to the reliability of the device and the repeatability of the tests, further investigations will be carried out to understand the influence of fire retardants on the fire behavior of thermosetting and thermoplastic-based composites considered for aeronautical applications.

Acknowledgements

The work presented in this study is the result of the RIN (Réseau d'Intérêt Normand) project AEROFLAMME (Behaviour of **AERO**nautical Composites under **FLAM**me and **ME**chanical Loading) financed by the Normandy Region and the FEDER (European Regional Development Fund).

References

[1] A. P. Mouritz and A. G. Gibson, “Fire Tests for Composites,” in *Fire Properties of Polymer Composite Materials*, Springer Netherlands, 2007.

[2] ISO 2685, “Resistance to fire in designated fire zones,” 1998.

[3] AC 20-135 chg 1, “Powerplant Installation and Propulsion System Component Fire Protection Test Methods, Standards and Criteria,” 2018.

[4] S. LeNeve, “AC 20-135 / ISO 2685 Fire tests on components used in fire zones. Comparison of gas burner to oil burner.,” presented at the International Aircraft Materials Fire Test WG, Atlantic City, 2008.

[5] A. Hörold, B. Schartel, V. Trappe, M. Korzen, and J. Bünker, “Fire stability of glass-fibre sandwich panels: The influence of core materials and flame retardants,” *Composite Structures*, vol. 160, pp. 1310–1318, Jan. 2017, doi: 10.1016/j.compstruct.2016.11.027.

[6] A. P. Mouritz *et al.*, “Review of fire structural modelling of polymer composites,” *Composites Part A: Applied Science and Manufacturing*, vol. 40, no. 12, pp. 1800–1814, 2009, doi: 10.1016/j.compositesa.2009.09.001.

[7] N. Grange, K. Chetehouna, N. Gascoin, A. Coppalle, I. Reynaud, and S. Senave, "One-dimensional pyrolysis of carbon based composite materials using FireFOAM," *Fire Safety Journal*, vol. 97, pp. 66–75, Apr. 2018, doi: 10.1016/j.firesaf.2018.03.002.

[8] S. I. Stoliarov, S. Crowley, R. E. Lyon, and G. T. Linteris, "Prediction of the burning rates of non-charring polymers," *Combustion and Flame*, vol. 156, no. 5, pp. 1068–1083, 2009, doi: 10.1016/j.combustflame.2008.11.010.

[9] E. Schuhler, A. Coppalle, B. Vieille, J. Yon, and Y. Carpier, "Behaviour of aeronautical polymer composite to flame: A comparative study of thermoset- and thermoplastic-based laminate," *Polymer Degradation and Stability*, vol. 152, pp. 105–115, 2018, doi: 10.1016/j.polymdegradstab.2018.04.004.

[10] A. G. Gibson, W. N. B. Wan-Jusoh, and G. Kotsikos, "A propane burner test for passive fire protection (PFP) formulations containing added halloysite, carbon nanotubes and graphene," *Polymer Degradation and Stability*, vol. 148, pp. 86–94, 2018, doi: 10.1016/j.polymdegradstab.2018.01.013.

[11] P. Tranchard *et al.*, "Fire behaviour of carbon fibre epoxy composite for aircraft: Novel test bench and experimental study," *Journal of Fire Sciences*, vol. 33, no. 3, pp. 247–266, 2015, doi: 10.1177/0734904115584093.

[12] B. Schartel, J. K. Humphrey, A. G. Gibson, A. Hörold, V. Trappe, and V. Gettwert, "Assessing the structural integrity of carbon-fibre sandwich panels in fire: Bench-scale approach," *Composites Part B: Engineering*, vol. 164, pp. 82–89, May 2019, doi: 10.1016/j.compositesb.2018.11.077.

[13] A. Petit, B. Vieille, A. Coppalle, F. Barbe, and M.-A. Maaroufi, "High temperature behaviour of PPS-based composites for aeronautical applications: Influence of fire exposure on tensile and compressive behaviors," presented at the 20th International Conference on Composite Materials, 30th 2015.

[14] D. Blond, B. Vieille, M. Gomina, and L. Taleb, "Correlation between physical properties, microstructure and thermo-mechanical behavior of PPS-based composites processed by stamping," *Journal of Reinforced Plastics and Composites*, vol. 33, no. 17, pp. 1656–1668, 2014, doi: 10.1177/0731684414541846.

[15] J. Zhang, M. A. Delichatsios, T. Fateh, M. Suzanne, and S. Ukleja, "Characterization of flammability and fire resistance of carbon fibre reinforced thermoset and thermoplastic composite materials," *Journal of Loss Prevention in the Process Industries*, vol. 50, pp. 275–282, Nov. 2017, doi: 10.1016/j.jlp.2017.10.004.

[16] E. Schuhler, B. Lecordier, J. Yon, G. Godard, and A. Coppalle, "Experimental investigation of a low Reynolds number flame jet impinging flat plates," *International Journal of Heat and Mass Transfer*, vol. 156, p. 119856, Aug. 2020, doi: 10.1016/j.ijheatmasstransfer.2020.119856.

[17] M. McKinnon, Y. Ding, S. I. Stoliarov, S. Crowley, and R. Lyon, "Pyrolysis model for a carbon fiber/epoxy structural aerospace composite," *Journal of Fire Sciences*, vol. 35, pp. 1–26, 2016, doi: 10.1177/0734904116679422.

[18] J. B. Henderson and T. E. Wiecek, "A Mathematical Model to Predict the Thermal Response of Decomposing, Expanding Polymer Composites," *Journal of Composite Materials*, vol. 21, no. 4, pp. 373–393, 1987, doi: 10.1177/002199838702100406.

[19] M. Balat-Pichelin, J. F. Robert, and J. L. Sans, "Emissivity measurements on carbon–carbon composites at high temperature under high vacuum," *Applied Surface Science*, vol. 253, no. 2, pp. 778–783, Nov. 2006, doi: 10.1016/j.apsusc.2006.01.007.

[20] D. B. P. Boulet A. Collin, Z. Acem, G. Parent, "On the influence of the sample absorptivity when studying the thermal degradation of materials," *Materials*, vol. 8, no. 8, pp. 5398–5413, 2015.

[21] E. P. Scott and J. V. Beck, "Estimation of Thermal Properties in Epoxy Matrix/Carbon Fiber Composite Materials," *Journal of Composite Materials, vol. 26, 1: pp. 132-149. , First Published Jan 1,* vol. 26, no. 1, pp. 132–149, 1992.

[22] Robert Gardon, "An instrument for the direct measurement of intense thermal radiation," *Review of Scientific Instruments*, vol. 24, no. 5, pp. 366–369, 1953, doi: https://doi.org/10.1063/1.1770712.

[23] G. M. Carlomagno and A. Ianiro, "Thermo-fluid-dynamics of submerged jets impinging at short nozzle-to-plate distance: A review," *Experimental Thermal and Fluid Science*, vol. 58, pp. 15–35, Oct. 2014, doi: 10.1016/j.expthermflusci.2014.06.010.

[24] H. Ingason and U. Wickström, "Measuring incident radiant heat flux using the plate thermometer," *Fire Safety Journal*, vol. 42, no. 2, pp. 161–166, Mar. 2007, doi: 10.1016/j.firesaf.2006.08.008.

[25] U. Wickström, J. Sjöström, and J. Anderson, "Measuring incident heat flux and adiabatic surface temperature with plate thermometers in ambient and high temperatures," *Fire and Materials*, vol. 43, pp. 51–56, 2019.

[26] C. M. Rippe and B. Y. Lattimer, "Full-field surface heat flux measurement using non-intrusive infrared thermography," *Fire Safety Journal*, vol. 78, pp. 238–250, Nov. 2015, doi: 10.1016/j.firesaf.2015.10.004.

[27] H. Jo, J. L. King, K. Blomstrand, and K. Sridharan, "Spectral emissivity of oxidized and roughened metal surfaces," *International Journal of Heat and Mass Transfer*, vol. 115, pp. 1065–1071, Dec. 2017, doi: 10.1016/j.ijheatmasstransfer.2017.08.103.

[28] S. W. Churchill and H. H. S. Chu, "Correlating equations for laminar and turbulent free convection from a vertical plate," *International Journal of Heat and Mass Transfer*, vol. 18, no. 11, pp. 1323–1329, Nov. 1975, doi: 10.1016/0017-9310(75)90243-4.